The Role of Implanter Parameters on Implant Damage Generation: an Atomistic Simulation Study

J. Singer[1,3,5], M. Jaraíz[2], P. Castrillo[2], C. Laviron[3], N. Cagnat[4], F. Wacquant[4], O. Cueto[3], A. Poncet[5]

[1]NXP Semiconductors, 17 rue des Martyrs, Grenoble, 38054, France. julien.singer@cea.fr
[2]University of Valladolid, Valladolid, 47011, Spain
[3]CEA-Léti, MINATEC, 17 rue des Martyrs, Grenoble, 38054, France
[4]STMicroelectronics, 850 rue Jean Monnet, Crolles, 38926, France
[5]Lyon Nanotechnologies Institute (UMR-CNRS 5270), Villeurbanne, 69621, France

Abstract. In this article we use atomistic process simulation to study the effect of some implanter parameters on damage accumulation for two types of implanters: a batch tool with a spot ion beam and a single-wafer tool with a ribbon beam. The studied parameters are the scanning speed, the wheel rotation speed and the beam diameter for the former, and the scanning speed and the beam width for the latter. We kept constant not only the species, dose and energy, but also the average dose rate, managed by the beam current, the wafer temperature (T). In such conditions damage accumulation is expected to be constant. However we show that beam focalization has a strong impact, because it affects the instantaneous dose rate. We define the instantaneous dose rate as the dose rate seen by a point of the wafer while it passes through the beam. Its effects on damage accumulation are comparable to those of wafer T and average dose rate.

Keywords: Ion implantation, Si, atomistic simulation, damage accumulation, beam focalization, instantaneous dose rate.
PACS: 61.72.uf, 61.80.Az, 61.80.Jh, 85.40.Ry

INTRODUCTION

Ion implantation generates cascades of damage within the silicon crystal. Interstitial-Vacancy (IV) Frenkel pairs accumulate and form highly damaged (but still crystalline) regions, conventionally called amorphous pockets (AP's) [1]. When the defects concentration exceeds a threshold, the silicon becomes amorphous. The amorphization by ion implantation depends directly on species, energy, dose, tilt and rotation. But other parameters affect it: for instance, the effects of implant T and average dose rate (DR_{avg}) are both significant [2,3]. In the present study, the effect of other parameters specific to two different ion implanter types is also investigated. The batch (BH) tool processes 13 wafers at once, is placed on a wheel which spins around, and is scanned over the spot ion beam. Scanning speed $V_{scan(BH)}$, wheel rotation speed $V_{rot(BH)}$ and beam diameter $D_{beam(BH)}$ (focalization) can vary. The single-wafer (SW) tool scans the wafer over a rectangular, ribbon ion beam. Scanning speed $V_{scan(SW)}$ and beam width $W_{beam(SW)}$ (focalization) will be studied. Fig.1 explains schematically the beam movements on the wafer for both implanter types.

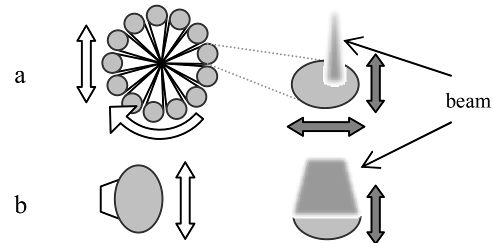

FIGURE 1. Schematic representation of a BH implanter and its beam on the wafer (a) and of a SW tool and its beam (b). Open arrows represent the wafer(s) movements in the implanter (the beam is fixed) and filled arrows show the resulting movements of the beam with respect to the wafer.

THEORY AND MODELING

Let's consider a point on the wafer. Each time it passes through the ion beam, there is a pulse of implantation. For the SW tool, the number of pulses coincides with the number of passes (fig.2 (a)). For the BH tool, the implantation consists of a series of bursts of short pulses (fig.2 (b)). Each wheel revolution produces one pulse and each scan leads to one burst. Fig.2 (c) schematically explains for the BH tool that

due to $D_{beam(BH)}$, any point on the wafer is exposed several times during a scan, which results in bursts of pulses.

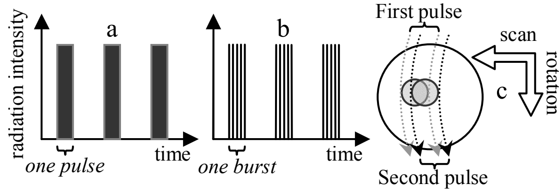

FIGURE 2. Implantation modes for (a) SW and (b) BH implanters. (c) The BH tool, for each wheel revolution a pulse of implantation is performed on the wafer.

The relevant implanter characteristics affecting the characteristics of pulses are presented in table 1 for the BH tool and in table 2 for the SW tool.

TABLE 1. Implanter parameters of the BH tool.

Name	Parameter description	Reference value
$D_{wheel(BH)}$	wheel diameter	130 cm
$V_{rot(BH)}$	rotation speed	15 rnd.s^{-1}
$D_{scan(BH)}$	scanning amplitude	35 cm
$I_{beam(BH)}$	beam current	5 mA
$D_{beam(BH)}$	beam diameter	5 cm
$V_{scan(BH)}$	scanning speed	5 cm.s^{-1}

TABLE 2. Implanter parameters of the SW tool.

Name	Parameter description	Reference value
$D_{scan(SW)}$	scanning amplitude	35 cm
$I_{beam(SW)}$	beam current	5 mA
$L_{beam(SW)}$	beam length	30 cm
$W_{beam(SW)}$	beam width	3 cm
$V_{scan(SW)}$	scanning speed	20 cm.s^{-1}

DR_{avg} is usually considered. It is calculated as:

$$DR_{avg} = \frac{Dose_{tot}}{Time_{tot}}, \quad (1)$$

and is proportional to the beam current I_{beam}. However we can also define the instantaneous dose rate DR_{inst}. This is the dose rate during a short time, for instance within a pulse:

$$DR_{inst} = \frac{\delta(dose)}{\delta(time)}, \quad (2)$$

where δ(dose) is the dose implanted during the short time δ(time).

In this study we use the atomistic process simulation tool DADOS. It has been proven to be reliable due to physical models implementation [4]. In particular, ion implantation is modeled in two stages. First the Marlowe code generates a cascade of IV pairs for each implanted ion using the Binary Collision Approximation [5]. The cascades are then implanted one after the other. The number of cascades N_{casc} that are simulated depends on the simulated surface $Surf_{simul}$:

$$N_{casc} = Dose_{tot} \cdot Surf_{simul}. \quad (3)$$

The time Δt_{casc} between two cascades depends on DR_{inst}:

$$\Delta t_{casc} = \frac{1}{DR_{inst} \cdot Surf_{simul}}. \quad (4)$$

During this relaxation time the diffusion of interstitials (I's) and vacancies (V's) and their recombination are simulated at the implant T, which is considered to be constant. DADOS allows the simulation of ion implantation as a series of short pulses. The input parameters are described in table 3. They are enough to define the implantation profiles of fig.2. The calculus of these parameters is based on the implanter parameters presented in table 1 and table 2.

TABLE 3. Parameters used as inputs in DADOS.

Abbreviation	Parameter description
$N_{casc/pulse}$	number of cascades per pulse
t_{pulse}	pulse duration
Δt_{pulse}	time between two pulses
$N_{pulses/burst}$	number of pulses per burst
Δt_{burst}	time between two bursts

It is also possible to simulate a time-uniform implantation. In that case DR_{inst} equals DR_{avg} and Δt_{casc} is then:

$$\Delta t_{casc} = \frac{1}{DR_{avg} \cdot Surf_{simul}}. \quad (5)$$

Finally at any time of the process DADOS allows access to atomistic data, that are not experimentally available.

RESULTS

For both implanters I_{beam} is kept constant in order not to modify the DR_{avg}. Moreover D_{scan} is taken bigger than the wafer diameter (300 mm), which is in turn the value retained for $L_{beam(SW)}$ of the SW tool. Implant conditions were chosen close to amorphization limit in order to highlight the effect of all these parameters. If any, the transition values presented here can not be generalized. For each implant condition a specific study should be performed in order to see if a variation would be critical or not.

For the batch tool the realistic range of values for $V_{scan(BH)}$ is between 1 and 30 cm.s^{-1}. For a too low $V_{scan(BH)}$, $N_{pulses/burst}$ becomes too high, and it is better for uniformity to do several scans instead of only one or two. The results of $V_{scan(BH)}$ variation on damage accumulation are depicted in fig.3 (a). Damage accumulation is given as a volume fraction, with respect to the reference value. The trend we observe is that there is not an abrupt transition between an amorphizing and a non-amorphizing range.

Although $V_{rot(BH)}$ is usually fixed on a given machine, we wondered how its variation would affect damage accumulation. For uniformity reasons, the value of $V_{rot(BH)}$ would not go down under 1 rnd.s^{-1}. The upper value of 35 rnd.s^{-1} will probably not be

exceeded. In this range no significant variations of amorphization is observed, as it is shown in fig.3 (b).

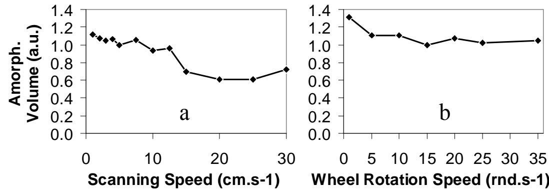

FIGURE 3. Effect of (a) $V_{scan(BH)}$ and (b) $V_{rot(BH)}$ on damage accumulation.

Finally, the variation of $D_{beam(BH)}$ results from focalization. As $D_{beam(BH)}$ decreases (resp. increases), pulses are shorter (resp. longer) but more (resp. less) "intense" – bigger (resp. smaller) $N_{casc/pulse}$. Thus DR_{inst} is directly increased (resp. decreased). Realistic values for $D_{beam(BH)}$ variations are between 1 and 15 cm. The results are represented in fig.4. We observe that $D_{beam(BH)}$ variations can result in drastic changes on damage accumulation during implantation.

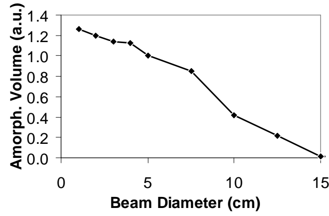

FIGURE 4. Effect of $D_{beam(BH)}$ (focalization) on damage accumulation.

Now we analyze the results for the SW tool. Plausible values for $V_{scan(SW)}$ are contained within the 10 – 40 $cm.s^{-1}$ range. Fig.5 (a) shows that the amorphization of silicon is not affected by $V_{scan(SW)}$. $L_{beam(SW)}$ being equal to the wafer diameter, only $W_{beam(SW)}$ is affected by the focalization of the rectangular, ribbon ion beam of the SW implanter.

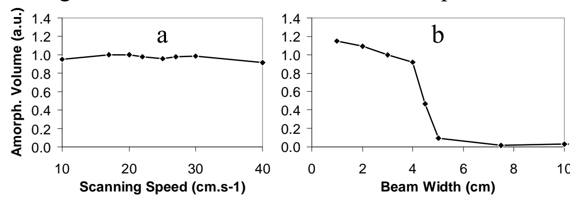

FIGURE 5. Effect of (a) $V_{scan(SW)}$ and (b) $W_{beam(SW)}$ (focalization) on damage accumulation.

The effect of the beam focalization on damage accumulation is quite remarkable, as seen in fig.5 (b). There exists a threshold value (dependent on the other parameters and on the implant conditions) over which the amorphization volume decreases suddenly.

DISCUSSION

We brought to the fore that the beam focalization has a strong impact on damage accumulation, while V_{scan} and–for the BH tool–$V_{rot(BH)}$ do not affect it. The reason can be found by examining the DR_{inst} evolution. In fig.6 the evolution of DR_{inst} for a BH tool is plotted as a function of the implanter parameters. It appears that DR_{inst} only depends on $D_{beam(BH)}$. Indeed the same number of cascades is implanted within a shorter pulse.

For the SW tool the assessment is the same. As it is shown in fig.7, DR_{inst} only depends on $W_{beam(SW)}$ and not on $V_{scan(SW)}$.

And indeed, for both implanter types, plotting the damage accumulation as a function of DR_{inst} (fig.8) leads to a threshold effect, similar to the behavior observed with DR_{avg} variations during time-uniform implants [2].

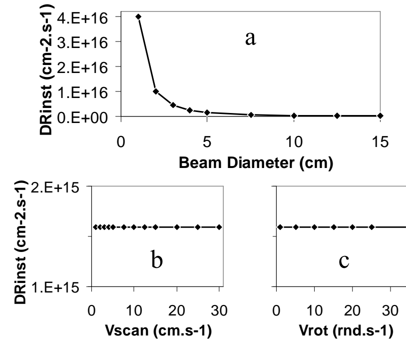

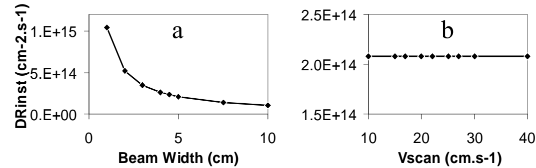

FIGURE 6. Evolution of DR_{inst} with (a) $D_{beam(BH)}$, (b) $V_{scan(BH)}$ and (c) $V_{rot(BH)}$, for the BH tool.

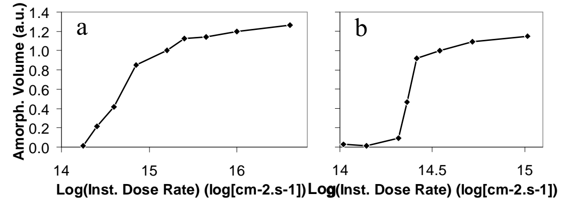

FIGURE 7. Evolution of DR_{inst} with (a) $W_{beam(SW)}$ and (b) $V_{scan(SW)}$, for the SW tool.

FIGURE 8. Damage accumulation as a function of DR_{inst} for the BH tool (a) and for the SW tool (b).

The DR_{inst} parameter has a drastic effect on damage accumulation because it affects the size of AP's after a pulse. In order to facilitate the analysis we will now stay with a damage below the amorphization threshold and look at the number of I's that are present within AP's. Big AP's ($N_{I's}$ + $N_{V's}$ $\geq$ 40) form during implantation by the overlap of several cascades, as

shown in fig.9. As we saw earlier, IV pairs recombination rate within AP's depends on their size. Bigger AP's are more stable, i.e. recombination is less efficient [6]. Fig.10 (a) shows that recombination in AP's resulting from a higher number of cascades hardly occurs in comparison with dynamic recombination of few cascades. Fig.10 (b) highlights that these are the biggest AP's which remain while the smallest underwent recombination.

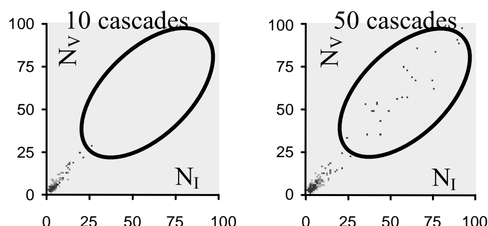

FIGURE 9. This graph plots the AP's composition histogram. The X and Y axes represent the number of I's and V's, respectively, in AP's. Each point represents a type of AP, containing X I's and Y V's. The grey level is representative of the concentration of (I's+V's). More big AP's are present when several cascades overlap.

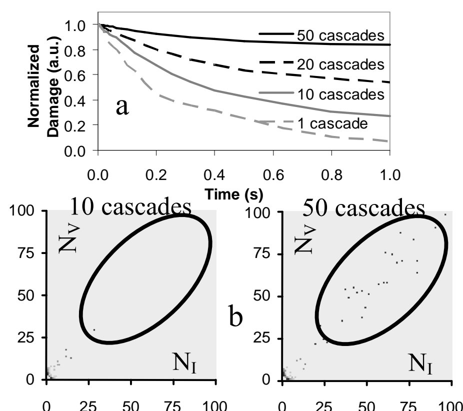

FIGURE 10. (a) Normalized I's dose in AP's as a function of relaxation time at room T, for different initial defect densities. (b) Comparison with fig.9 shows that unlike small AP's, the big ones did not undergo recombination after 1s relaxation at room-T.

Thus at the end of a pulse, more AP's remain that are bigger if DR_{inst} is increased. This is plotted in fig.11. In this condition, even if relaxation happens between each pulse, damage accumulation will be more important with a higher DR_{inst}.

CONCLUSION

Our atomistic process simulations concerned two types of implanters, a BH tool with a spot ion beam and a SW tool with a ribbon ion beam. We studied the effect of some implanter parameters on damage

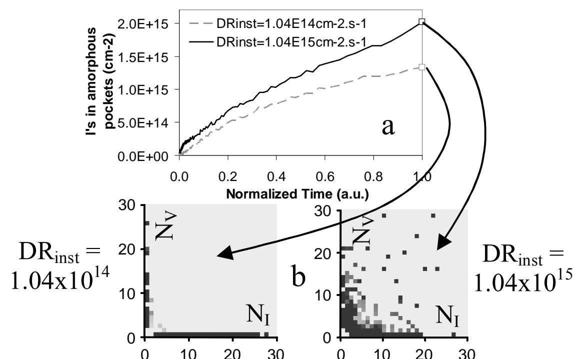

FIGURE 11. (a) The curves represent the evolution of the number of interstitials present in AP's as a function of normalized time (0 is the beginning of the pulse and 1 is its end). (b) Moreover AP's histograms show that with the lower DR_{inst} (larger $W_{beam(SW)}$) there are less AP's containing both I's and V's. This is evidence that recombination was more efficient.

accumulation during the implantation. The studied parameters are $V_{scan(BH)}$, $V_{rot(BH)}$ and $D_{beam(BH)}$ for the BH tool, and $V_{scan(SW)}$ and $W_{beam(SW)}$ for the SW tool. We kept constant not only the implanted species, dose and energy, but also the DR_{avg} (and thus I_{beam}) and the wafer T. In these conditions our simulations showed that only beam focalization ($D_{beam(BH)}$ and $W_{beam(SW)}$) did affect damage accumulation. We introduced the DR_{inst}, which is the dose rate seen by a point of the wafer while it passes through the beam. It is directly related to beam focalization. DR_{inst} has a strong impact on damage accumulation, at the same level than the DR_{avg} or the wafer T. Though beam focalization depends on the energy, it may vary from one implanter to the other, the user having no control on it. However it is also important to consider this parameter for experiments concerning amorphization and implantation defects studies.

REFERENCES

1. Caturla, M.-J., Díaz de la Rubia, T., Marqués, L. A., and Gilmer, G. H., *Phys. Rev. B* **54**, 16683-16695 (1996).
2. Schultz, P. J., Jagadish, C., Ridgway, M. C., Elliman, and R. G., Willimas, J. S., *Phys. Rev. B* **44**, 9118-9121 (1991).
3. Goldberg, R. D., Williams, J. S., and Elliman, R. G., *Nucl. Instr. Meth. in Phys. Res. B* **106**, 242-247 (1995).
4. Jaraíz, M., Gilmer, G. H., Poate, J. M., and Díaz de la Rubia, T., *Appl. Phys. Letters* **68**, 409-411 (1996).
5. Robinson, M. T., and Torrens, I. M., *Phys. Rev. B* **9**, 5008-5024 (1974).
6. Mok, K. R. C., Jaraíz, M., Martin-Bragado, I., Rubio, J. E., Castrillo, P., Pinacho, R., Barbolla, J., and Srinivasan, M. P., *J.Appl. Phys.* **98**, 046104 (2005).